sustainability

MDPI

Article

Feasibility Study of School-Centred Peer-to-Peer Energy Trading with Households and Electric Motorbike Loads

Lerato Paulina Molise [1], Jason Avron Samuels [1] and Marthinus Johannes Booysen [1,2,3,*]

[1] Department of Industrial Engineering, Stellenbosch University, Stellenbosch 7600, South Africa
[2] Department of E&E Engineering, Stellenbosch University, Stellenbosch 7600, South Africa
[3] Department of Computing and Technology, Uganda Christian University, Mukono P.O. Box 4, Uganda
* Correspondence: mjbooysen@sun.ac.za

Abstract

South Africa faces high energy costs, highlighting the urgent need for sustainable and cost-effective energy solutions. This study investigates the design of a cost-effective photovoltaic energy system that maximises savings and revenue for the school through energy trading. In this study, the school trades with 14 neighbouring households and 125 electric motorbikes. This research first applies Latin Hypercube Sampling to explore the solution space and determine which system parameters have a significant impact on supply reliability, investment costs, revenue and savings. Optimal solutions are generated using Non-Dominated Sorting Genetic Algorithm II for a range of system scenarios. Following this, the most promising scenario is selected and applied to 53 schools in the Western Cape. The results show that number of panels strongly correlates with both supply reliability and revenue, thus reducing the break-even years, while battery capacity affects investment costs and, to some extent, break-even years. Among the configurations tested, scenarios where schools traded with both households and electric motorbikes, particularly when both included their own battery systems, achieved the most favourable financial performance for the school, with break-even periods of less than five years under sufficient roof area and improved reliability for the external entities, with an average improvement of 60%. These findings demonstrate that peer-to-peer energy trading between schools and communities can enhance the financial feasibility and sustainability of decentralised solar systems, offering a scalable model for improving energy access and affordability in South Africa and possibly other developing countries.

Keywords: energy trading; micro-grid; schools; electric mobility; households; energy storage systems; photovoltaic (PV); Non-Dominated Sorting Genetic Algorithm II; Latin Hypercube Sampling

Check for updates

Academic Editors: Vincenzo Gallelli and Rosolino Vaiana

Received: 24 December 2025
Revised: 14 January 2026
Accepted: 15 January 2026
Published: 18 January 2026

Copyright: © 2026 by the authors. Licensee MDPI, Basel, Switzerland. This article is an open access article distributed under the terms and conditions of the Creative Commons Attribution (CC BY) license.

1. Introduction

The global energy landscape is undergoing substantial transformation, driven by the need to mitigate climate change and ensure energy security. This urgency is reflected in Sustainable Development Goal 7, which calls for "universal access to affordable, reliable, sustainable and modern energy" by 2030 [1]. Achieving this has proven to be a challenge, particularly in sub-Saharan Africa, which accounts for 75% of the world's energy access deficit [2]. This research focuses on a case study of South Africa, a country that also faces the energy challenges that are prevalent across sub-Saharan Africa.

South Africa's electricity challenges mainly include persistent grid instability, high electricity costs, and high carbon emissions [3,4]. Since 2008, scheduled power cuts have been implemented to mitigate the energy access deficit. In 2024, the frequency of power cuts declined, with the national electricity supplier projecting decreased power cuts going forward [5]. However, the costs remain high. South African electricity tariffs increased by 190% from 2014 to 2024, far exceeding the inflation rate of 5.2% over the same period [6]. In addition, the national electricity supply remains highly carbon-intensive due to its continued reliance on coal-fired power generation [4].

Institutions such as schools are affected by these challenges. Rapidly increasing tariffs place a financial burden on schools, diverting limited resources from core educational purposes [7]. Furthermore, power outages disrupt academic activities and hinder effective school functioning. The low- to non-fee-paying schools are disproportionately affected by this, as they primarily rely on government funding, which typically increases at a slower rate than electricity tariffs [8]. While renewable energy sources such as photovoltaic (PV) solar are available, the associated installation costs remain a major constraint for already resource-limited schools.

Beyond schools, households across South Africa are also affected by high electricity costs and an unreliable supply, although the impacts vary across income groups. High-energy-consuming households often face significantly higher tariffs. For example, high-income households in the Stellenbosch municipality pay nearly three times more per kilowatt-hour (kWh) than the lowest consumers [9]. This results in households, especially those with high income, resorting to photovoltaic battery energy storage systems (PV/BESS) [10]. However, limited storage capacity often results in unused excess energy [8], reducing the gains that come with PV/BESS. Low-income households, on the other hand, are already faced with financial constraints, and they remain exposed and solely reliant on the expensive and unreliable public power supply. Despite differences in income, all residential areas need more sustainable solutions to combat these energy challenges.

In addition to renewable energy, various demand-side and efficiency-based strategies have been explored to reduce electricity costs in buildings. One such solution is controlling electric water heaters based on predicted demand instead of simply maintaining a constant temperature [11]. Hughes and Larmour [12] analyse other methods, encouraging retrofits in existing residential areas to meet water heating requirements using solar water heaters and heat pumps. Hughes and Larmour [12] further proposes government-subsidised scrapping programs to encourage the replacement of inefficient appliances like refrigerators. All of the proposed solutions are costly for the majority, necessitating further research into methods to alleviate the impacts of this energy crisis.

Although these challenges are central to buildings, it is also important to consider the broader emission landscape and how other sectors interact with this energy system. The transport sector remains a major contributor to air pollution, with road transport accounting for approximately 23% of global emissions [13]. This has driven the global transition from internal combustion engines (ICEs) to electric vehicles (EVs), with EVs accounting for 18% of global car sales in 2023, up from 2% five years prior [14]. However, in South Africa, charging EVs from a coal-powered grid undermines these environmental benefits [15]. Pretorius et al. [16] found that EVs charged on coal-based electricity produce higher CO_2 emissions than ICE vehicles, while also adding pressure to an already fragile grid [13]. In order for South Africa to seamlessly integrate EVs despite its challenges, it is crucial to consider shared sustainable energy solutions.

1.1. Research Questions

Building on the preceding discussion, this research is structured around the following research questions.

1. What range of system configurations allows school-based solar-battery microgrids to achieve energy autonomy while financially sustaining themselves through electricity trading?
2. How do different system design and operational choices influence the technical and financial performance of the school-centred microgrids?

1.2. Scope

This study assesses the feasibility of school-centred PV/BESS energy trading systems under realistic external load scenarios. The analysis prioritises exploration of the design space and examination of system-level trade-off between total investment cost and net cash flow within a local energy-trading framework. Households and electric motorbikes are used as external entities to determine whether the school and systems can support additional loads of comparable magnitude.

1.3. Contribution

This study introduces an optimisation framework in which schools act as energy producers, supplying households and electric motorbikes within a local trading market. It evaluates PV/BESS sizing using Non-Dominated Sorting Genetic Algorithm II (NSGA-II) and explicitly incorporating reliability constraints that are largely absent from existing P2P trading studies. In addition, the inclusion of electric motorbikes adds flexible-demand participants that can engage in energy trading independent of the grid. By using empirically derived consumption profiles from South African schools, households and electric motorbikes, this study further fills a critical geographic and contextual gap in quantifying trading prices, resource requirements, and payback periods for a school-centred energy trading model.

2. Literature Review

2.1. Foundations of Energy Trading

Energy trading has emerged as one of the financial incentives offered to encourage adoption of renewable energy [17,18] to address global climate change, energy security and sustainable economic development challenges [18]. In energy trading, consumers are given the chance to sell back their energy to the grid, becoming both consumers and producers (prosumers). However, these are often limited by the need to maintain grid stability. Norouzi et al. [19] discuss different government-driven pricing policies used to mitigate this challenge. Their study found that these policies can shape the techno-economic performance of PV/BESS; therefore, solutions that align with both the grid's operational and consumers' needs are required.

While Norouzi et al. [19] focus on improving consumer outcomes through alternative government-regulated pricing policies, other studies shift away from tariff-based regulation by adopting peer-to-peer (P2P) energy trading frameworks. In P2P energy trading, energy is exchanged directly between prosumers and consumers, allowing more flexibility in solutions that are mutually beneficial to the entities involved. For example, Nguyen et al. [20] model a local P2P market where clearing prices are determined based on supply–demand interactions within regulated rates, enabling households to trade in highly favourable conditions.

2.2. Optimisation-Based Approaches on PV/BESS and Energy Trading

A substantial body of literature formulates PV/BESS planning and operations as optimisation problems. They typically use mixed-integer linear programming (MILP) to capture discrete investment decisions alongside energy flows.

2.2.1. MILP-Based PV-BESS Optimisation Under Energy Trading Frameworks

The literature formulated PV-BESS systems' planning and operation as optimisation problems which could be solved using MILP. Within this group, several studies explicitly embedded local energy trading within the optimisation structure.

Yaldız et al. [21] present an MILP formulation for joint PV/BESS sizing and P2P energy trading in residential systems. Importantly, their contribution goes beyond operational scheduling: the optimisation simultaneously determines optimal PV/BESS capacities while accounting for capital replacement and maintenance costs over the project lifetime, which is twenty-five years. The authors compared P2P trading with grid participation, showing that the former leads to higher profits and shorter payback periods. However, this study assumes perfect information and does not include entities beyond household loads. Furthermore, while battery replacement costs are included, battery degradation is not dynamically linked to operational decisions, potentially underestimating the costs and overstating the system size.

Nguyen et al. [20] extend MILP-based optimisation to a large-scale P2P trading community of 500 households. Their study focuses on operational decision-making rather than sizing; that is, charging, discharging, consuming, buying, and selling energy rather than determining the best size of the PV/BESS. Their key contribution lies in modelling a realistic P2P market clearing mechanism, including trading margins, feed-in tariffs, retail prices, and heterogeneous household configurations (PV-only, battery-only, PV+battery, and none). The authors show that participation in P2P trading does not uniformly benefit all actors; in particular, households with battery-only configurations may achieve lower financial savings than households without any distributed generation due to storage costs.

2.2.2. Battery-Centred Optimisation and the Role of Degradation

While the discussed energy-trading studies treat batteries as ideal storage devices, a parallel strand of literature focuses on battery degradation as a first-order economic driver, even in the absence of trading. Wu et al. [22] explicitly addressed this gap by proposing a two-layer MINLP optimisation framework that jointly considers battery capacity operation and long-term degradation. Their contribution lies in embedding both cyclic aging and time-dependent aging models into the optimisation problem, allowing battery degradation to directly influence life-cycle cost. The results demonstrate that neglecting degradation costs leads to systematic underestimation of life-cycle costs and insufficient battery sizing. Incorporating degradation mechanisms shifts the optimal solution towards larger battery capacities, which operate at shallower depth-of-discharge and thereby extend battery lifetime.

Hassan et al. [23] analyse grid-connected PV/BESS under feed–in tariffs and time-varying electricity prices using a year-long, half-hourly optimisation framework based on real residential PV generation and load data. The optimisation results demonstrate that batteries should be charged during low-cost periods, either from excess PV or cheap grid imports, and discharge when prices are high to maximise revenue. The study also found that time-varying tariffs significantly outperform flat-rate tariffs for prosumers. A sensitivity analysis of battery capacity reveals diminishing marginal economic returns beyond an optimal storage size (approximately 3 kWh for the case study considered), highlighting the importance of informed battery sizing rather than excessive capacity expansion.

2.2.3. Decentralised Energy Trading Beyond Conventional Microgrids

Finally, a study by Samuel et al. [24] broadens the discussion to decentralised energy trading architectures by proposing a blockchain-based decentralised energy system for Sub-Saharan Africa. The authors combine energy trading, incentive mechanisms, and reliability-aware cost evaluation through the introduction of a Blockchain-levelised energy cost. This explicitly incorporates reliability metrics such as full rate and service level into cost assessment. While the proposed architecture offers a novel perspective compared to the approaches discussed earlier, it is primarily applied at the planning level and remains illustrative rather than operational. As a result, system sizing and real–time operational dispatch are not modelled in detail, limiting direct comparability with MILP-based micro-optimisation studies that focus on operational realism.

2.3. Research Gaps

The major gaps identified in the literature are

- No studies examine schools or public buildings as energy suppliers in P2P trading.
- There is limited integration of P2P trading with detailed system sizing under unreliable grid conditions.
- No study evaluates school-to-community energy trading under affordability and reliability constraints.

3. Methodology

This section describes the modelling and optimisation framework used to evaluate the feasibility of a school-centred PV/BESS and its ability to trade energy with external entities. The approach combines half-hourly energy flow simulation with exploratory sampling and multi-objective optimisation to assess how different system configurations influence financial returns and supply reliability. At the core of the framework is an evaluation function that simulates three years of PV power generation, battery behaviour, energy distribution, revenues, savings, and reliability for the school and external entities.

3.1. Data

This study made use of four datasets: solar irradiance, schools, electric motorbikes and household energy demand. The school demand dataset, sourced from Samuels et al. [25], provides half-hourly electricity consumption data for 53 schools in the Western Cape; the data were collected through smart meters over a one-year period. Household electricity demand was obtained from Eskom et al. [26], which contains half-hourly consumption records for South African households across various regions from 1994 to 2014. Fourteen households with complete measurements for the year 2014 were selected for this study. One-minute electric motorbike load data from Stratford and Booysen [27] were aggregated to a half-hourly resolution to align with the other datasets. Finally, irradiance data was generated with System Advisory Model (SAM) [28], which simulated three years of global horizontal irradiance (GHI) for the Stellenbosch region. Figures 1–4 show boxplots for distributions of irradiance, schools, households, and electric motorbikes.

3.2. Modelling Procedures

3.2.1. Solar Generation

The solar panels modelled in this study each have a cost of R1 500 each, a rated output of 0.455 kW per panel, an efficiency of 20.6%, and a surface area of 2.21 m^2. Their performance is assumed to degrade linearly to 80% over 25 years, corresponding to an annual degradation rate of 0.8%. Using GHI data and the panel specifications, the solar energy generated at each timestep is calculated using Equation (1).

$$\begin{aligned} & E_{solar,t} = \min(P_{theoretical,t}, P_{rated}) \times \Delta t \times (1 - 0.008(y - 1)) \\ \text{where} \quad & P_{theoretical,t} = GHI_t \times A \times \eta \times N \\ & P_{rated,t} = P_{panel} \times N \end{aligned} \tag{1}$$

In this set of equations, $\Delta t = 0.5\,h$, $P_{theoretical,t}$ represents the theoretical power output under the given irradiance, and $P_{rated,t}$ is the rated output of installed panels. GHI_t is irradiance in kW/m^2 every 30 min, A is the panel area in m^2, η is the panel efficiency, N is the number of panels, $P_{panel} = 0.455\,kW$, and y is the simulation year.

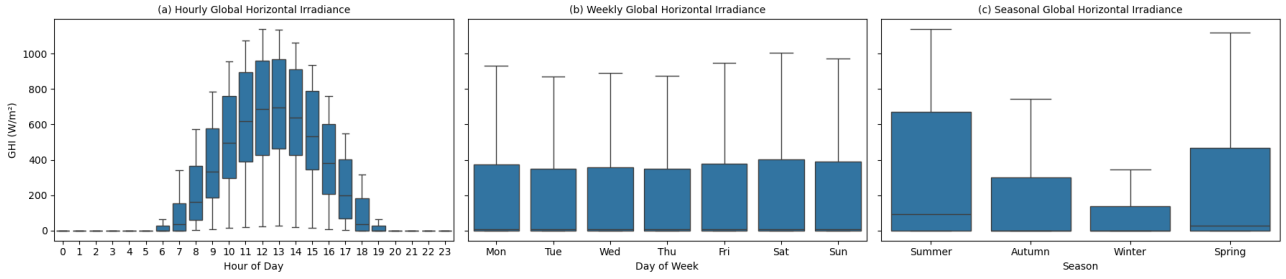


Figure 1. Distribution of global horizontal irradiance (GHI) across (**a**) hours of the day, (**b**) days of the week, and (**c**) seasons.

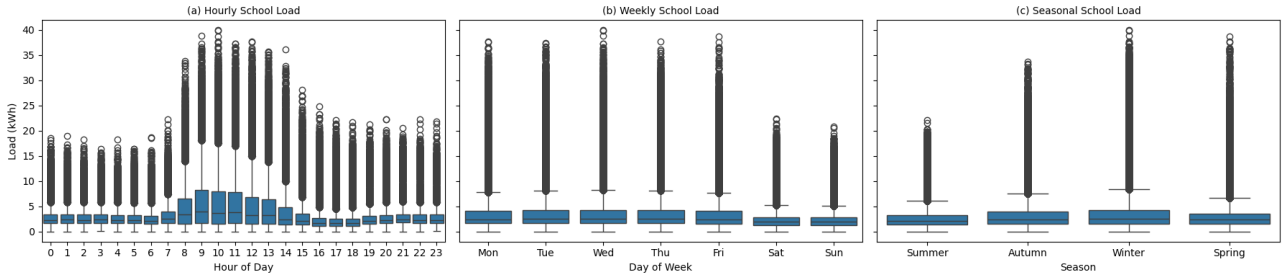


Figure 2. Distribution of school electricity demand across 53 schools by (**a**) hours of the day, (**b**) days of the week, and (**c**) seasons.

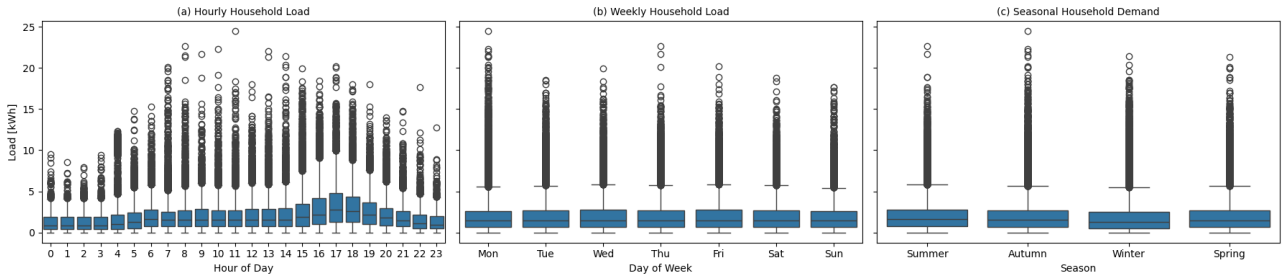


Figure 3. Distribution of aggregated household electricity demand for 14 households across (**a**) hours of the day, (**b**) days of the week, and (**c**) seasons.

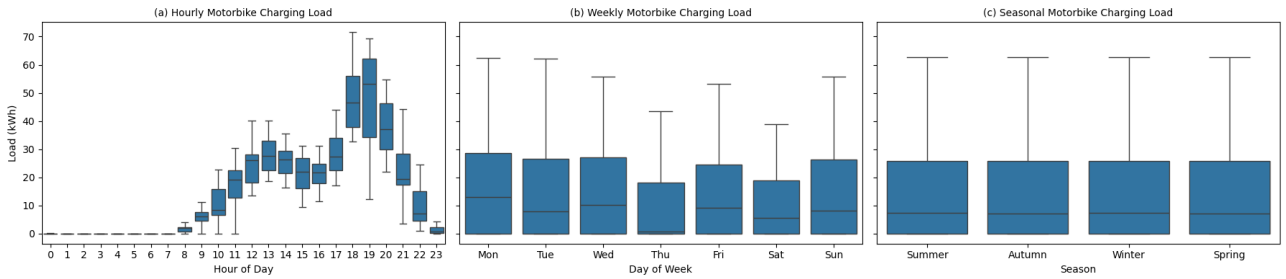


Figure 4. Distribution of charging demand for 125 electric motorbikes across (**a**) hours of the day, (**b**) days of the week, and (**c**) seasons.

3.2.2. Battery Energy Storage System

The Battery Energy Storage System (BESS) is based on Lithium Iron Phosphate $LiFePO_4$ battery modules with the following specifications: a total capacity of 5 kWh, a usable capacity of 4 kWh, and a cost of R14 000 per module. The charge and discharge efficiencies, η_c and η_d, are both 0.95, with a charge rate of 0.7 C and a discharge rate of 0.9 C. Each battery module degrades to 75% after 4000 cycles or 10 years, assuming operating temperatures between −20 °C and 45 °C. To model its behaviour over time, the State of Charge (SOC) at any timestep is defined by Equation (2).

$$\mathrm{SOC_t} = \frac{\mathrm{SOC_{t-1}} + \eta_c P_{\mathrm{charge,t}} - \frac{1}{\eta_d}\mathrm{P_{discharge,t}}}{\mathrm{P_n \times N}} \times 100 \quad (2)$$

where $\mathrm{P_{charge,t}}$, $\mathrm{P_{discharge,t}}$, $\mathrm{P_0}$ and N denote the charging power, the discharging power, the initial capacity of a single battery module, and the number of modules in the system, respectively. The SOC at t = 0 is assumed to be 100%, after which it is constrained between 20% and 95% to extend the battery's lifespan [29]. At each charging and discharging event, partial cycles are accumulated as shown in Equation (3). Charging events are limited by the effective usable capacity of the battery defined by Equation (4). $\mathrm{P_t}$ and $\mathrm{P_0}$ refer to the capacity at time t and the initial capacity, respectively.

$$\mathrm{cycle_t} = \frac{\Delta \mathrm{SOC_t}}{2 \times (0.95 - 0.2)} \quad (3)$$

$$\begin{aligned} \mathrm{P_t} &= \mathrm{P_0} e^{-\mathrm{kn}} \\ \text{where } \mathrm{k} &= \frac{-\ln(0.75)}{4000}, \\ \mathrm{n} &= \sum_{0}^{\mathrm{t}} \mathrm{cycle_t} \end{aligned} \quad (4)$$

3.3. Performance Measures

The performance of the optimisation framework is evaluated using three core performance metrics used during optimisation and a set of complementary performance metrics. The core performance metrics are total investment costs, net cash flow, and school supply reliability. Total investment represents the upfront capital expenditure for system deployment. Net cash flow represents the sum of revenues from electricity trading and savings resulting from elimination of grid electricity purchase. School supply reliability is imposed as a hard constraint to ensure there will be an uninterrupted electricity supply to the school under off-grid operation. The complementary performance indicators are excess energy, break-even period, and external entity supply reliability.

Savings are evaluated using a time-of-use (TOU) tariff structure applied to schools and revenue using renewable energy export TOU applied to traded electricity, both obtained from Stellenbosch Municipality [9]. The tariff defines peak, standard, and off-peak periods that vary by season and day of the week, with distinct rates for high-demand (winter) and low-demand (summer) periods. Prices are based on the municipal tariff schedule because it represents a regulatory-permissible benchmark for electricity transactions within the study context. The renewable export tariffs are priced below the equivalent grid purchase tariff, ensuring economic benefits for the participating entities while maintaining the competitive advantage that comes with P2P trading. Electricity tariffs were assumed to increase by 10% annually, with adjustments applied each July. Net cash flow was

subsequently discounted to present value to account for inflation. The mathematical formulations of the savings, investment costs and reliability are given in Equations (5)–(7).

$$\text{Average Savings} = \frac{6 \cdot F \cdot \sum_{y=1}^{3}\left(1.1^{y\text{-}1} + 1.1^{y}\right) + C \cdot \left(\sum_{t=0}^{8689}\left(E(t) \cdot 1.1^{y\text{-}1}\right) + \sum_{t=8689}^{17520}\left(E(t) \cdot 1.1^{y}\right)\right)}{3} \quad (5)$$

$$C_{inv} = C_{PV} + C_{bat} + C_{invtr} + C_{elec} + C_{mech} \quad (6)$$

$$R_{school} = \frac{1}{3}\sum_{y=1}^{3}\frac{E_{met}^{y}}{E_{demand}^{y}} \times 100 \quad (7)$$

In Equation (5), E(t) denotes the electrical energy supplied at times step t, F denotes fixed monthly charges, and C denotes the applicable unit cost depending on TOU. Equation (6) defines the total investment cost as the sum of PV module acquisition, battery acquisition cost (bat), inverter cost (invtr), electrical wiring system cost (elec), and mounting system cost (mech). The wiring and mounting system cost are modelled as functions of the number of installed PV panels consisting of a fixed base cost and a component proportional to PV capacity, reflecting mounting structures, wiring, and installation labour requirements. Equation (7) computes school supply reliability as the ratio of met electrical energy demand to total electrical energy demand, averaged across the three simulated years.

3.4. Evaluate Function

The evaluate function shown in Algorithm 1 simulates the operation of the school-centered PV/BESS over a three-year period at half-hourly resolution. Demand is assumed to be constant for all three entities, while GHI changes each year are all simulated for a non-leap year. For a given system configuration, it simulates solar power generation, battery degradation, energy dispatch, financial performance, and supply reliability for both the school and external entities. The same evaluation function is used for both sampling and optimisation. For sampling, the inputs are the number of panels, number of battery modules, demand factor, and operating hours, while for optimisation, the number of battery modules and number of panels are considered.

Algorithm 1 Evaluate function for a given PV/BESS configuration

Require: Number of panels, Number of battery modules, demand profiles, GHI data
Initialise cumulative revenue, savings, solar generated, demand, unmet demand
for year = 1 to 3 **do**
  for each timestep *t* **do**
    Compute $E_{solar,t}$, $D_{school,t}$, $D_{external,t}$
    if $E_{solar,t} < D_{school,t}$ **then**
      Discharge battery to meet school demand
      Discharge battery to meet external demand
    else
      Charge battery with available solar
      Supply school using solar
      Supply external demand using remaining solar and/or battery
    end if
    Update reliability, revenue, savings, unmet demand, and battery cycles
  end for
end for
  return Average revenue, average savings, average net cash flow, investment cost, payback period, school reliability, external reliability, average solar generated, average excess energy generated

3.5. Exploratory Sampling Using Latin Hypercube Sampling

Latin Hypercube Sampling (LHS) was used to explore the full design space and quantify the relationship between system design variables and performance indicators prior to optimisation. LHS ensures a uniform sampling of the multidimensional input space. Four decision variables were sampled: the number of solar panels, the number of battery modules, the school operating hours, and a demand factor representing improvements in energy efficiency. The sampled ranges were as follows:

- Number of solar panels: $40 \leq N_p \leq 700$.
- Number of battery modules: $5 \leq N_b \leq 600$.
- Operating hours per day on school days: $N_h \in \{6, 8, 11, 24\}$.
- Demand reduction factor: $0.7 \leq \alpha \leq 1.0$.

Each sampled configuration was evaluated using Algorithm 1. The resulting dataset formed the basis of the correlation analysis presented in Section 4.1, which was used to identify the most influential design variables and inform the optimisation formulation.

3.6. Multi-Objective Optimisation Using NSGA-II

The system design problem involves competing objectives, as increasing system size improves net cash flow and reliability but also raises investment costs. To capture these trade-offs, the problem was formulated as a multi-objective optimisation problem, where a set of pareto-optimal solutions are generated. This was solved using Non-Dominated Sorting Genetic Algorithm II (NSGA-II), a widely used evolutionary algorithm known for its computational efficiency and suitability with a small number of objectives [30,31]. NSGA-II was selected due to its ability to maintain solution diversity while converging towards a set of optimal solutions.

The optimisation was implemented in Python version 3.12.6 using the `pymoo` library within the same software environment. A population size of 30 and 30 offspring per generation were used. Sensitivity tests were conducted by increasing both the population size and number of offspring to 100; however, no material changes were observed in the resulting pareto front. The smaller population was, therefore, used to retain computational efficiency. Integer random sampling ensured feasible combinations of solar panels and battery modules within the defined bounds. Each candidate solution was evaluated using Algorithm 1. The optimisation problem is defined as follows. Let

- $X = (x_1, x_2) = (N_{\text{panels}}, N_{\text{batteries}})$.
- $f_1(X)$ denote the total investment cost.
- $f_2(X)$ denote the average net cash flow.
- $S^{(y)}(X)$ denote the school supply reliability in year $y \in \{1,2,3\}$.

$$\begin{aligned} \min \quad & (f_1(X), -f_2(X)) \\ \text{s.t.} \quad & 100 - 10^{-6} - S^{(y)}(X) \leq 0, \quad \forall y \\ & 40 \leq x_1 \leq 500 \\ & 5 \leq x_2 \leq 300 \end{aligned} \tag{8}$$

Following optimisation, the pareto-optimal solutions were ranked using the Technique for Order of Preference by Similarity to Ideal Solution (TOPSIS). TOPSIS is one of the most widely used MCDM methods [32], and is favoured for its simplicity, practicality, and computational efficiency [32,33]. TOPSIS ranks alternatives based on their closeness to the positive ideal solution, which maximises benefits and minimises costs, and their distance from the negative ideal (anti-ideal) solution [32]. For this study, TOPSIS was used as follows:

Let i = 1, 2, . . . , 900 index the set of pareto-optimal configurations generated by NSGA-II for a given scenario. Each configuration i is characterised by multiple performance metrics and inputs, the two objectives central to this problem are investment cost I_i and the average NCF_i. The decision matrix is therefore defined as follows:

$$X = \begin{bmatrix} I_1 & NCF_1 \\ I_2 & NCF_2 \\ \vdots & \vdots \\ I_{900} & NCF_{900} \end{bmatrix} \tag{9}$$

The two were then normalised and weighted as shown in Equation (11). A slightly higher weight was assigned to investment cost to reflect budget sensitivity in school-based installations.

$$\bar{I}_i = w_I \frac{I_i}{\sqrt{\sum_{k=1}^{900} I_k^2}}, \tag{10}$$

$$\overline{NCF}_i = w_{NCF} \frac{NCF_i}{\sqrt{\sum_{k=1}^{900} NCF_k^2}} \tag{11}$$

where $w_I = 0.6$ and $w_{NCF} = 0.4$. The positive ideal solution represents the configuration with the lowest-weighted and normalised investment cost and the highest-weighted and normalised average net cash flow, while the negative (anti-ideal) solution represents the opposite extreme. These are defined by Equations (12) and (13)

$$I^+ = \min(\bar{I}_i), \qquad NCF^+ = \max(\overline{NCF}_i) \tag{12}$$

$$I^- = \max(\bar{I}_i), \qquad NCF^- = \min(\overline{NCF}_i) \tag{13}$$

The Euclidean distances of each configuration from the positive and negative ideal solutions are computed as D_i^+ and D_i^-.

$$D_i^+ = \sqrt{(\bar{I}_i - I^+)^2 + (\overline{NCF}_i - NCF^+)^2}, \tag{14}$$

$$D_i^- = \sqrt{(\bar{I}_i - I^-)^2 + (\overline{NCF}_i - NCF^-)^2} \tag{15}$$

The relative closeness, C_i of each configuration to the ideal solution is then calculated by Equation (16), after which the configurations are ranked in descending order of C_i. The configuration with the highest C_i is selected as the most balanced solution for the given scenario.

$$C_i = \frac{D_i^-}{D_i^+ + D_i^-} \tag{16}$$

3.7. Scenario Analysis

The optimisation was performed under six scenarios:

1. School sells to households.
2. School sells to electric motorbikes.
3. School sells to both households and electric motorbikes.
4. School sells to households with a battery each.
5. School sells to electric motorbikes with an extra battery in addition to the one they have.
6. School sells to households and electric motorbikes with a battery.

The best scenario was then selected and applied to 53 schools in the Western Cape, and the results are compared.

4. Results and Discussion

This section presents the results derived from the simulation described in the Methodology. The analysis begins by examining how system inputs shape financial and energy supply reliability outcomes. It then evaluates the performance of energy trading between one school and external entities; 14 households and 125 electric motorbikes, both individually and jointly. Additional scenarios incorporating battery storage for external entities are also assessed. Building on these findings, this section identifies the most balanced system configuration using the TOPSIS method for each scenario. Finally, the solution is assessed for scalability by applying optimisation across 53 schools with varying annual electricity consumption.

4.1. Correlation Analysis of System Inputs and Performance Indicators

Factors that can influence the costs, revenue, and eventually break-even for this system, as discussed in the Methodology, are varying number of panels, number of battery modules, operating hours for the school energy system, and improving the efficiency of the system. In the model, the efficiency of the system is improved by introducing a demand factor to the demand per timestep. A range of inputs are generated using LHS and the outputs are presented in Figure 5. The correlations are discussed below.

4.1.1. Number of Panels

The number of panels shows a strong positive correlation with supply reliability, revenue, and average net cash flow, as well as a moderate negative correlation with break-even years. Increasing the number of panels increases daytime energy generation, which improves supply reliability and increases revenue.

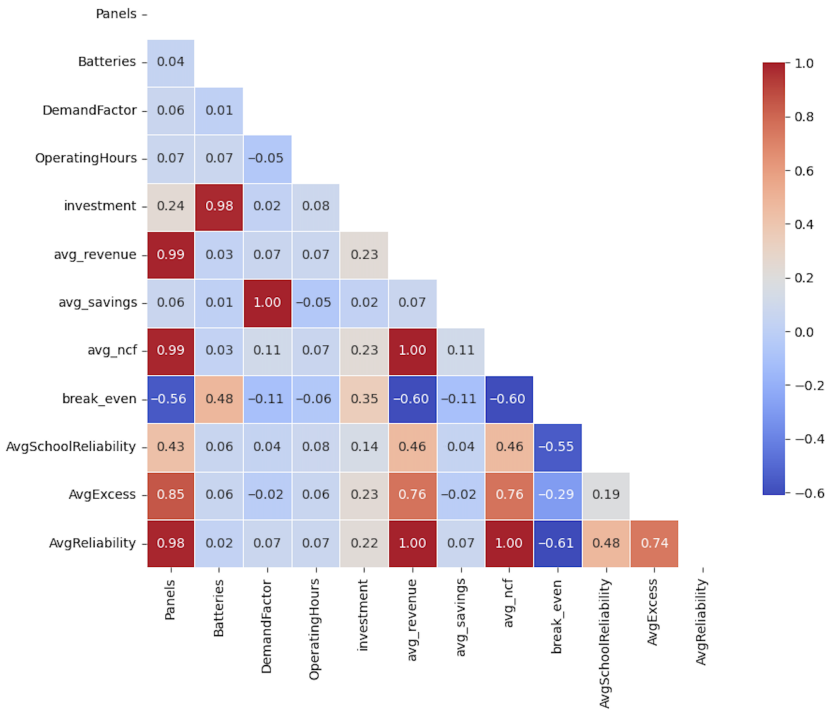


Figure 5. Correlation between key input variables generated through LHS and system performance indicators.

4.1.2. Number of Battery Modules

Battery capacity is strongly correlated with investment costs and moderately correlated with break-even years. Given that each battery module costs R14 000 compared to R1 500 per

solar panel, batteries are expected to have the strongest impact on overall system cost. However, battery storage remains necessary to achieve 100% reliability for the school. Since the school primarily operates during daylight hours, when solar power is available, extensive storage capacity is not required. This suggests that configurations in which residential areas and electric motorbikes have dedicated storage should be considered, as their peak demand periods indicate a greater benefit from increased storage capacity.

4.1.3. Demand Factor

The demand factor shows a strong correlation with savings but little association with other performance metrics. As expected, reducing the school's energy demand lowers electricity expenditure, even under grid-connected operation. However, because savings have a limited influence on net cash flow, the demand factor has an insignificant effect on the break-even period. Consequently, efficiency improvements at the school should only be pursued where they incur no additional costs, such as through behavioural interventions.

4.1.4. Operating Hours

Operating hours show no significant correlation with the performance metrics, indicating that variations in school operating time have minimal influence on overall system performance. Although reduced operating hours would be expected to lower energy consumption, most of the hours removed occur outside normal school hours, when energy demand is already low. Consequently, varying operating hours is not recommended as an effective intervention.

4.1.5. Other Correlations

Other moderate-to-strong correlations were observed between the performance metrics. A strong correlation exists between reliability and excess energy, as achieving higher reliability typically requires larger system sizes, which in turn lead to increased excess energy, particularly when storage capacity is limited. In addition, break-even period shows a strong correlation with average revenue and net cash flow, indicating that savings contribute only a small share of the overall net cash flow.

Given that variations in demand factor and operating hours have a limited influence on system performance indicators, the optimisation focuses solely on the number of solar panels and battery modules as the primary decision variables.

4.2. Exploring Optimal Energy-Trading Scenarios for One School Case Study

Figure 6 presents optimisation results for energy trading with households and electric motorbikes, both with and without additional external battery storage. Each point in the scatter plots represents a unique combination of solar panels and school-side battery modules generated by the NSGA-II optimisation described in the previous section. The x-axis shows the average net cash flow for three years (in thousand Rands), while the y-axis shows the corresponding total investment costs for that configuration. Each configuration is coloured according to the average excess energy produced over the three year period in MWh, using a colourmap where darker shades indicate lower excess energy and lighter shades indicate high excess energy. The dashed lines represent the break-even trend lines. Figure 6a,b show performance when energy trading with electric motorbikes and battery without providing a battery to the external entity, while (c) and (d) show equivalent comparisons when the electric motorbikes have an extra battery and each household has a battery. Figure 7 shows similar results but for energy trading with both entities, (a) without battery and (b) with battery. When comparing electric motorbikes and households without external storage, there are apparent (although not significant) differences in performance. For both entities, net cash flow increases with investment costs, but electric motorbikes

consistently achieve higher returns, reaching net cash flow values close to R700 000, whereas households converge around R650 000. This difference can be attributed to the electric motorbike daily energy profile in Figure 4, which exhibits peaks during the day and in the evening, creating more opportunities to absorb solar generation. In contrast, households peak in the evening, reducing their ability to utilise the excess daytime solar generated. Despite these differences, both scenarios yield similar payback periods, mostly between 7 and 8 years, reflecting the comparable annual consumption levels. The excess energy generated is also not significantly different.

Introducing a battery of the same capacity for the school to the external entities alters the system's performance most notably in electric motorbikes. This is because there are 125 electric motorbikes, while there are only 14 households, each with the same capacity of 5 kWh. With an additional battery, the electric motorbikes configurations achieve higher net cash flows, starting from R500 000 for investment costs, where the non-battery scenario reaches only R350 000. The payback periods for electric motorbikes with an extra battery start at less than 6 years compared to 7 years without an extra battery. In contrast, households exhibit only marginal improvements with the addition of a battery. The net cash flow shows only a difference of less than R50 000 and the payback period differing by less than a year for the same investment costs. Across all scenarios, there is substantial excess energy, often exceeding 150 MWh, especially when there is no extra storage. This surplus indicates potential for more revenue through sale of excess energy.

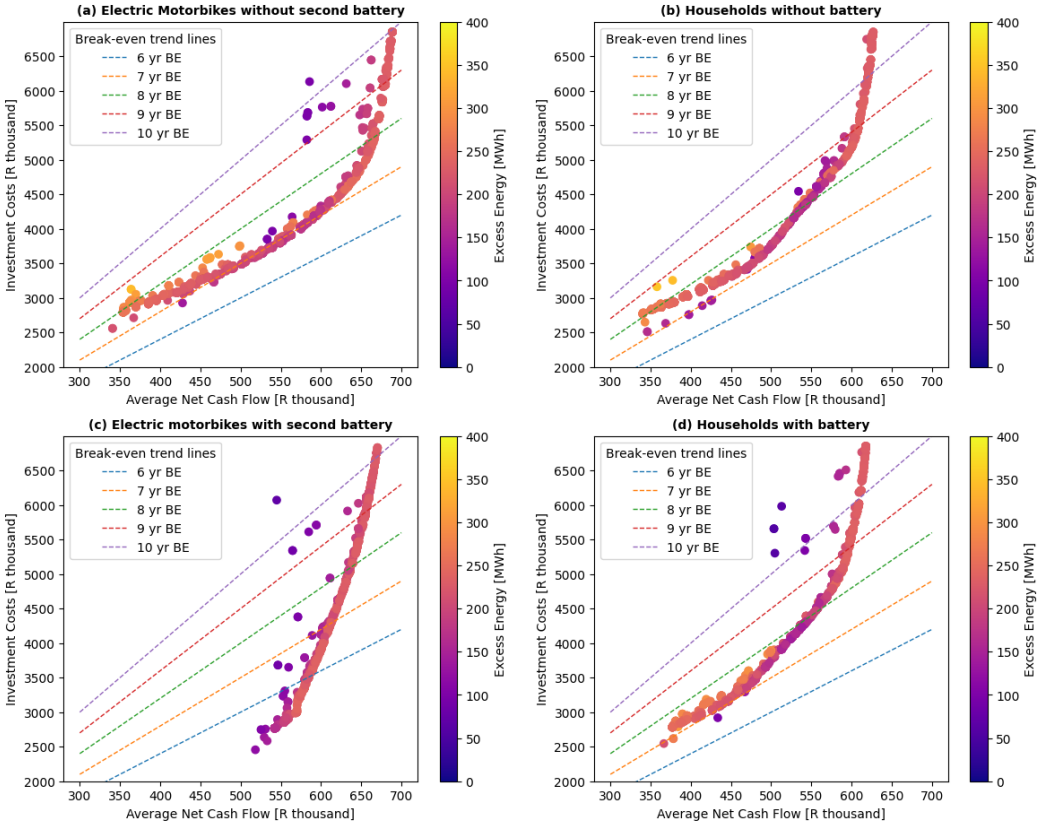


Figure 6. Investment costs vs. average net cash flow for system trading with (**a**) electric motorbikes without a second battery (**b**) households without battery, (**c**) electric motorbikes with an additional battery per motorbike, and (**d**) households with a single battery. Each point corresponds to a distinct combination of solar panels and school-side battery modules. The colour of each point corresponds to excess energy, while dashed lines indicate payback period trend lines.

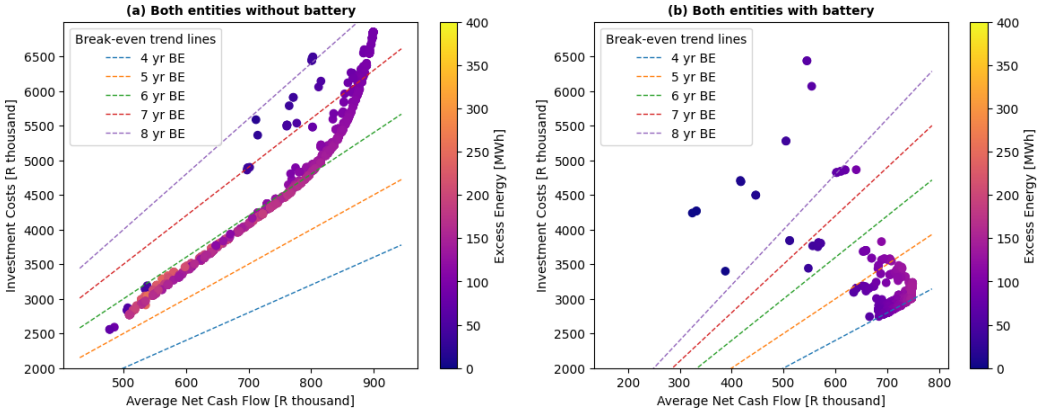


Figure 7. Investment costs vs. average net cash flow for system trading with (**a**) both entities without a battery and (**b**) both entities with a battery. Each point corresponds to a distinct combination of solar panels and school-side batter modules. The colour of each point corresponds to excess energy while dashed lines indicate payback period trend lines.

Figure 7 shows optimisation results for energy trading with both households and electric motorbikes. When both entities participate, the model identifies higher-performing configurations across the investment range, with net cash flow starting from R500 000 to as high as R900 000 compared to the highest net cash flow of R700 000 with single entities. Payback periods are also significantly reduced. Without a battery, most solutions have a payback period of less than 6 years compared to less than 5 years when the entities have a battery. The excess energy generated is also noticeably low—less than 150 MWh for most solutions. This might, in fact, be the most favourable scenario for the schools.

Table 1 summarises the best-performing configurations selected from each scenario using the TOPSIS method, which ranks the solutions based on investment cost and net cash flow. For each scenario, the table reports the number of panels and batteries, total investment costs, average annual revenue, net cash flow, payback period, external entity supply reliability, and average excess energy.

Table 1. Summary of optimal configurations showing system parameters, investment costs, revenues, net cash flows, break-even periods, supply reliability, and average excess energy over a three-year simulation period.

System	Number of Panels	Number of Batteries	Investment Costs	Avg Revenue	Avg Net Cash Flow	Payback Period	Supply Reliability	Avg Excess [MWh]
Electric motorbikes	372	102	R2 927 200	R311 730	R490 854	6 years 10 months	56%	137.85
Households	377	104	R2 970 950	R310 181	R426 245	7 years	55%	145.43
Electric motorbikes with an extra battery	463	61	R2 585 050	R417 016	R533 081	4 years 10 months	82%	144.64
Households with a battery	338	109	R2 919 300	R317 474	R433 538	6 years 9 months	59%	100.38
Households and Electric motorbikes	487	65	R2 725 450	R393 380	R509 444	5 years 4 months	40%	175.078
Households and Electric motorbikes with battery	517	65	R2 815 950	R588 478	R704 543	4 years	60%	94.85

The results show that the best financial performance comes from scenarios where the school trades with electric motorbikes or both entities, especially when battery modules are added. These cases achieve the highest net cash flows and the lowest payback period, driven by their ability to absorb the excess energy that is generated. However, the additional energy storage required in these scenarios would be purchased and maintained by the external entities, not the school. For this reason, a more conservative recommendation for the school is energy trading with both entities without external batteries, which still offers

a short payback period of just over 5 years while relying on infrastructure that the school controls. Furthermore, energy trading with households may require further investment in infrastructure for a system that is not constrained by the grid. This makes energy trading with electric motorbikes without an extra battery technically more viable to implement.

4.3. Is the Proposed Solution a One-Size-Fits-All? Performance Across 53 Schools in Western Cape

The preceding analysis focused on a single case study school, but the validation of feasibility of the proposed PV/BESS trading system depends on how it performs across different schools. To evaluate this, the optimisation framework was applied to 53 schools in the Western Cape, each with distinct average annual energy consumption, as summarised by [7]. The scenario discussed is when the schools sell to both external entities. This subsection compares the distribution of best solutions, the performance of each school's best configuration, and the resource requirements associated with achieving optimal results.

Figure 8 summarises the payback periods of the top 30 out of 900 solutions generated for each school. The boxplots reveal that while some schools cluster tightly around a single payback period, others exhibit a much broader spread. Schools with wider boxplots tend to achieve shorter median payback periods, whereas those with narrow boxplots generally display longer payback periods. A narrow boxplot indicates a constrained optimisation landscape in which only a limited set of configurations can satisfy the reliability requirement. Although schools with high annual energy consumption most frequently exhibit this restricted behaviour, several low-consumption schools show similar patterns, suggesting that factors beyond annual demand may play a role too.

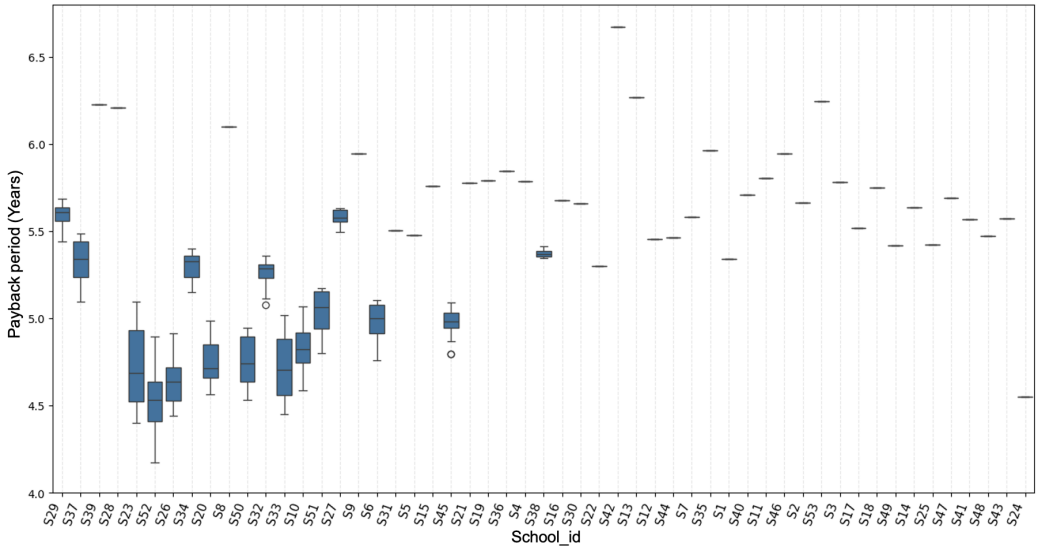


Figure 8. Boxplots for payback period for 53 schools trading energy with both external entities. The plots represent the top 30 solutions of 900 and the schools are sorted from low to high annual energy consumption.

To further understand the variability in performance, Figure 9 displays the best-performing configuration for each school, annotated with school reliability and coloured by excess solar energy. A clear difference emerges: smaller and mid-sized schools almost always achieve 100% school reliability and mostly show low payback periods, even though they generally generate more excess energy. On the other hand, schools with high annual energy consumption rarely achieve 100% school reliability because their energy needs exceed what capped PV/BESS sizes can sustain. These schools also produce less excess energy, meaning that nearly all their energy is absorbed.

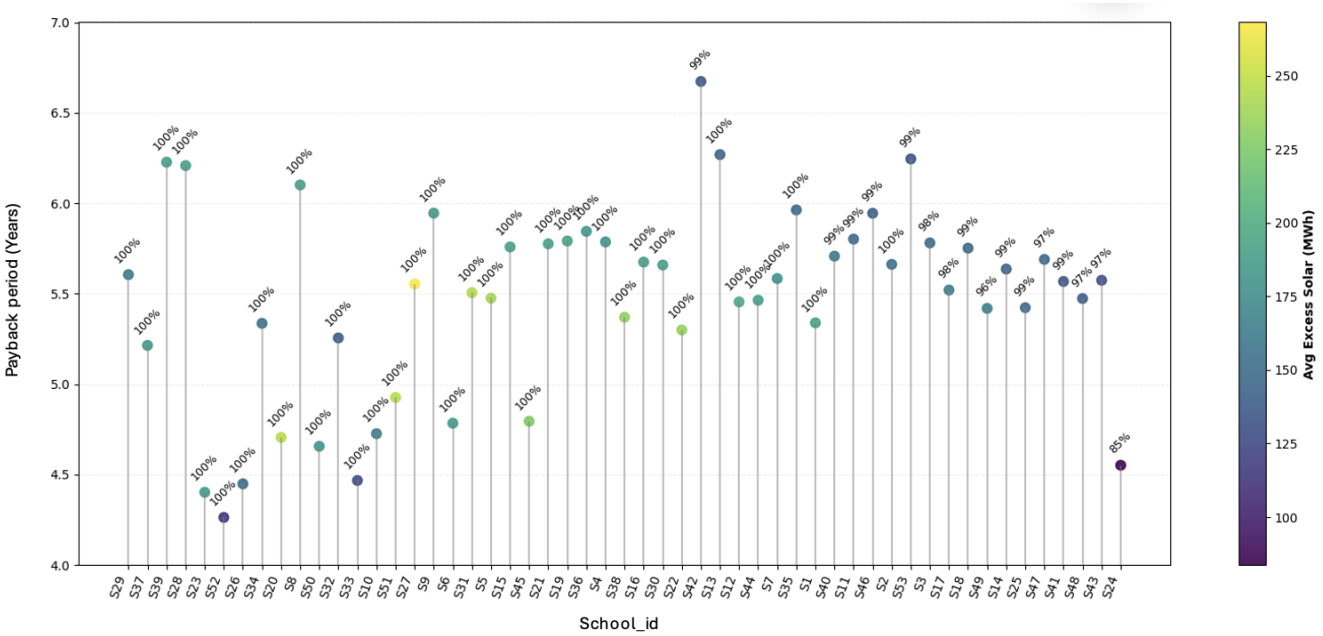


Figure 9. Optimal solutions for 53 schools energy trading with both external entities.

In practice, the deployment of PV systems in schools is often constrained by the available area, which can limit the feasibility of the cost-optimal configurations identified earlier. To account for this limitation, a complementary analysis is conducted using the same set of optimisation results. Rather than selecting cost-optimal solutions, the analysis identifies, for each school, the configuration that achieves the highest attainable school reliability while using the minimum number of PV panels. For most schools, this corresponds to 100% reliability, while 14 schools achieve reliability levels above 95% and one school attains approximately 85% reliability, as seen in Figure 9. This selection represents an area-constrained operating case and provides a lower bound on system performance when PV expansion is restricted and school reliability is prioritised.

Figure 10 shows the results of this analysis with the data points labelled 'number of panels, number of batteries' and the colour bar corresponding to the costs of investment. The results show that when PV capacity is constrained, achieving high reliability in schools becomes increasingly dependent on battery storage. As a result, payback periods increase relative to the cost optimal solutions discussed earlier, reflecting the higher investment required to compensate for limited solar generation. These results indicate that although high reliability can largely be maintained under area-limited conditions, doing so comes at a higher cost due to increased battery requirements. Consequently, if low investment costs are prioritised, the findings suggest that relaxing the school reliability target to less than 100% may be a more practical design choice than further increasing storage capacity. Nonetheless, when investment cost is not the primary constraint, the results still yield a payback period well below 10 years, with most schools averaging below seven years, indicating that the proposed framework remains economically viable.

Examining the number of panels and batteries required by each school reveals a broad pattern, though not a strict rule, in how resource needs scale across different schools. Many low-to-moderate-demand schools require fewer panels and relatively small battery units, while several higher-demand schools push toward upper limits of both components, especially with the 700-panel limit. However, notable exceptions exist: a few schools with comparatively low annual consumption still require disproportionately large battery and panel investments. These exceptions correspond to the schools that displayed narrow boxplots in Figure 8, further emphasising that their solution space is highly constrained

by their energy needs. This reinforces that resource need is reshaped not only by annual demand but by other structural factors.

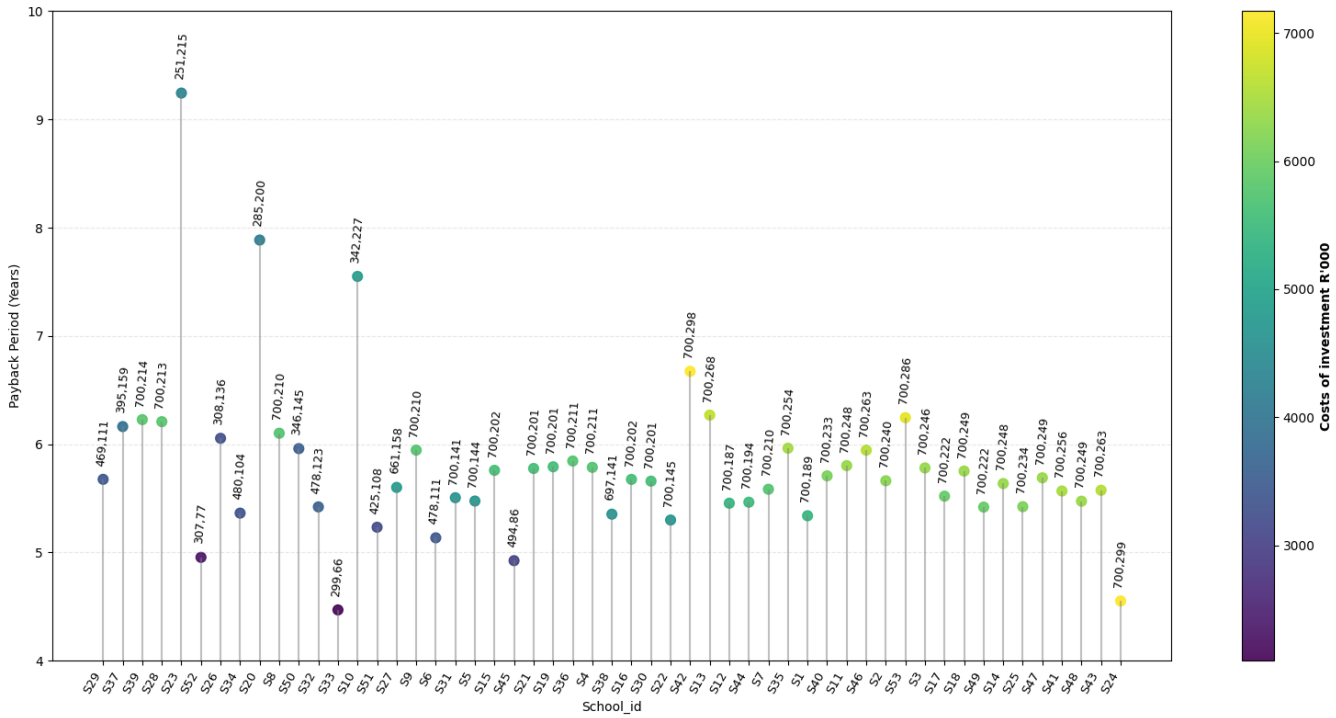


Figure 10. Payback period of minimum PV panel solutions meeting the reliability constraint for each school, with labels showing PV panel and battery counts and colour indicating investment cost.

The results reveal another way of categorising the schools into two groups beyond their annual energy consumption. The groups emerge from how tight or loose each school's feasible solutions are in Figure 8 and how high the resource requirements are as shown in Figure 10. Figure 11 compares the two groups' hourly load profiles: (a) schools with a wide range of solutions and (b) with a less flexible range of solutions. This comparison revealed a consistent pattern: the schools with flexible ranges have relatively lower daytime demand peaks and their demand begins to decline around 14:00 hrs, returning to close to early morning levels by mid-afternoon. In contrast, schools with narrow solution ranges exhibit a sharp morning increase, sustained elevated loads throughout the day, and only decrease to morning load levels at 15:00 hrs or later. This extended high-demand period places greater pressure on PV/BESS resources, limiting the number of possible configurations that would satisfy the reliability. Together, these observations suggest that the distinction between the schools is driven by their annual energy consumption demands, as well as shape and timing of their demand.

While different schools have different payback periods, the best payback periods are all less than 10 years. This suggests that the proposed solution has great potential for mitigating the impacts of the energy crisis in South African schools. With an in-depth study on grouping schools, the solution can be further optimised for different groups, thus making it more generally applicable. Factors such as school area may limit the number of panels used, so grouping the schools would undoubtedly allow better generalisation of the proposed solution.

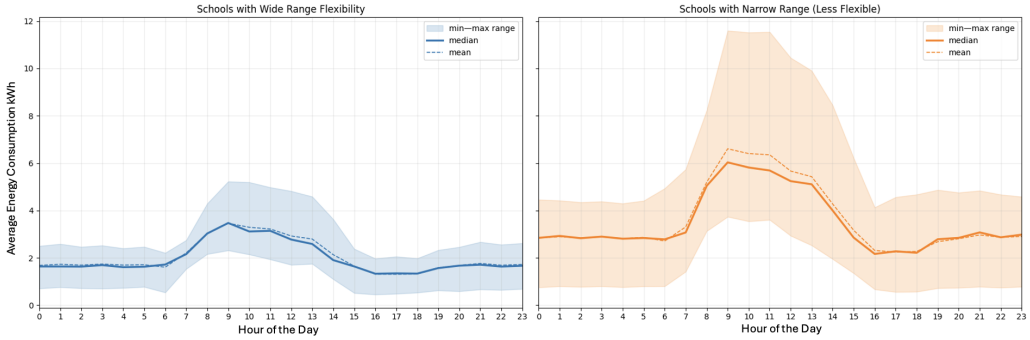


Figure 11. Shaded line graphs showing the spread of hourly energy consumption for two groups of schools grouped according to their optimisation results.

5. Conclusions

This study assessed the techno-economic viability of schools acting as energy prosumers via P2P trading with households and electric motorbikes. Results from the NSGA–II optimisation indicate that school-centred energy trading is feasible, with payback periods ranging from 4 to 7 years for larger PV system deployments and from 4 to 9 years for minimum PV configurations within reliability constraints. Trading with electric motorbikes consistently outperformed household scenarios due to motorbike energy consumption patterns being better aligned with the PV solar generation profile. Trading with both households and electric motorbikes yielded the highest financial returns, especially when batteries were added for each entity.

5.1. Limitations

This study is subject to several limitations. First, it relies on static household electricity demand profiles from 2014, as this was the most recent publicly available dataset with the necessary temporal resolution. Secondly, the school data is limited to anonymized schools in the Western Cape, preventing site-specific design considerations such as roof area or existing infrastructure layout. Moreover, the model does not include external low-voltage distribution infrastructure costs for connecting schools to households, as such costs would be highly site-specific. Additionally, the current battery degradation model does not account for temperature effects.

5.2. Future Work

Future work will extend the study using the proposed framework through the use of more detailed site-specific school data. In particular, data collection could be considered so that recommendations made for the framework could be more specific to the school groups. In addition, the framework can be extended to consider alternative trading partners such as nearby businesses or other community loads to further assess the role of schools as local energy hubs. Further refinement of the battery degradation representation may also be considered for long-term deployment analysis.

Author Contributions: Conceptualization, J.A.S. and M.J.B.; methodology, L.P.M.; software, L.P.M.; validation, L.P.M., J.A.S. and M.J.B.; formal analysis, L.P.M.; investigation, L.P.M.; resources, M.J.B.; data curation, L.P.M.; writing—original draft preparation, L.P.M.; writing—review and editing, L.P.M. and M.J.B.; visualization, L.P.M.; supervision, J.A.S. and M.J.B.; project administration, L.P.M., J.A.S. and M.J.B.; funding acquisition, J.A.S. and M.J.B. All authors have read and agreed to the published version of the manuscript.

Funding: This research was funded by The Centre for Renewable and Sustainable Energy Studies (CRSES).

Institutional Review Board Statement: Not applicable.

Informed Consent Statement: Not applicable.

Data Availability Statement: The simulation results are not publicly available but can be reproduced using the methods described in this study.

Conflicts of Interest: The authors declare no conflicts of interest.

Abbreviations

The following abbreviations are used in this manuscript:

BESS	Battery Energy Storage.
GHI	Global Horizontal Irradiance.
EV	Electric Vehicle.
ICE	Internal Combustion Engine.
kWh	Kilowatt-hour.
LHS	Latin Hypercube Sampling.
MWh	Megawatt-hour.
P2P	Peer-to-Peer.
PV	Photovoltaic.
SOC	State of Charge.
TOU	Time of Use.

References

1. United Nations Department of Economic and Social Affairs (UN DESA). Accelerating SDG 7 Achievement: Policy Briefs in Support of the First SDG 7 Review at the UN High-Level Political Forum 2018. 2018. Available online: https://sustainabledevelopment.un.org/content/documents/18041SDG7_Policy_Brief.pdf (accessed on 30 April 2025).
2. IEA. *Tracking SDG7: The Energy Progress Report, 2021*; IEA: Paris, France, 2021.
3. Avila, N.; Carvallo, J.P.; Shaw, B.; Kammen, D.M. The energy challenge in sub-Saharan Africa: A guide for advocates and policy makers. *Gener. Energy Sustain. Equitable Dev. Part* **2017**, *1*, 1–79.
4. Lawrence, A. Energy decentralization in South Africa: Why past failure points to future success. *Renew. Sustain. Energy Rev.* **2020**, *120*, 109659. [CrossRef]
5. Eskom. Eskom Suspends Loadshedding Following Recovery of Emergency Reserves—Summer Outlook Remains Unchanged, 2025. Available online: https://www.eskom.co.za/eskom-suspends-loadshedding-following-recovery-of-emergency-reserves-summer-outlook-remains-unchanged/ (accessed on 23 April 2025).
6. CSIR Energy Research Centre. Utility-Scale Power Generation Statistics in South Africa. 2024; p. 82. Available online: https://www.csir.co.za/sites/default/files/2025-09/Utility%20Statistics%20Report_Jan%202025_Final.pdf (accessed on 13 October 2025).
7. Samuels, J.A.; Michael-Ahile, T.; Booysen, M.T. Dataset on electricity usage measurement for lower-to-middle-income primary and secondary schools in Western Cape, South Africa. *Data Brief* **2025**, *59*, 111321. [CrossRef] [PubMed]
8. Michael-Ahile, T.; Samuels, J.A.; Booysen, M. Optimizing battery energy storage and solar photovoltaic systems for lower-to-middle-income schools amidst load-shedding. *Energy Sustain. Dev.* **2025**, *85*, 101675. [CrossRef]
9. Stellenbosch Municipality. Appendix 3: Stellenbosch Municipality Tariffs 2025/2026. 2025; pp. 3–4. Available online: https://stellenbosch.gov.za/download/appendix-3-draft-tariff-book-2025-2026/ (accessed on 30 August 2025).
10. The Competition Commission of South Africa. *Survey Findings on Renewable Energy Products Used by Households and Businesses*; Technical Report; The Competition Commission of South Africa: Pretoria, South Africa, 2024.
11. Booysen, M.; Engelbrecht, J.; Ritchie, M.; Apperley, M.; Cloete, A. How much energy can optimal control of domestic water heating save? *Energy Sustain. Dev.* **2019**, *51*, 73–85. [CrossRef]
12. Hughes, A.; Larmour, R. Assessment of the potential to improve the energy efficiency of household appliances in South Africa. *Energy Strategy Rev.* **2024**, *56*, 101595. [CrossRef]
13. Abraham, C.; Rix, A.; Ndibatya, I.; Booysen, M.J. Ray of hope for sub-Saharan Africa's paratransit: Solar charging of urban electric minibus taxis in South Africa. *Energy Sustain. Dev.* **2021**, *64*, 118–127. [CrossRef]
14. International Energy Agency. *Global EV Outlook 2024*; IEA: Paris, France, 2024. Available online: https://www.iea.org/reports/global-ev-outlook-2024 (accessed on 29 April 2025).
15. Booysen, M.J.; Abraham, C.J.; Rix, A.J.; Giliomee, J.H. Electrification of minibus taxis in the shadow of load shedding and energy scarcity. *S. Afr. J. Sci.* **2022**, *118*. [CrossRef]

16. Pretorius, B.; Wüst, J.; Strauss, J.; Bekker, J.; Booysen, M. Scheduling with mixed fleets to improve the feasibility of electric minibus taxis: A case scenario of South Africa. *J. Clean. Prod.* **2024**, *472*, 143512. [CrossRef]
17. United Nations Environment; Yale University; REN21. Renewable Energy and Energy Efficiency in Developing Countries: Contributions to Reducing Global Emissions. 2017. Available online: https://view.ckcest.cn/AllFiles/ZKBG/Pages/308/b5aa6d23b09c6b1b3e3796786c3319bcf88efaba.pdf (accessed on 15 September 2025).
18. Kabel, T.S.; Bassim, M. Literature review of renewable energy policies and impacts. *Eur. J. Mark. Econ.* **2019**, *2*, 28–40. [CrossRef]
19. Norouzi, F.; Shekhar, A.; Hoppe, T.; Bauer, P. Analysing the impact of the different pricing policies on PV-battery systems: A Dutch case study of a residential microgrid. *Energy Policy* **2025**, *204*, 114620. [CrossRef]
20. Nguyen, S.; Peng, W.; Sokolowski, P.; Alahakoon, D.; Yu, X. Optimizing rooftop photovoltaic distributed generation with battery storage for peer-to-peer energy trading. *Appl. Energy* **2018**, *228*, 2567–2580. [CrossRef]
21. Yaldız, A.; Gökçek, T.; Şengör, İ.; Erdinç, O. Optimal sizing and economic analysis of Photovoltaic distributed generation with Battery Energy Storage System considering peer-to-peer energy trading. *Sustain. Energy Grids Netw.* **2021**, *28*, 100540. [CrossRef]
22. Wu, Y.; Liu, Z.; Liu, J.; Xiao, H.; Liu, R.; Zhang, L. Optimal battery capacity of grid-connected PV-battery systems considering battery degradation. *Renew. Energy* **2022**, *181*, 10–23. [CrossRef]
23. Hassan, A.S.; Cipcigan, L.; Jenkins, N. Optimal battery storage operation for PV systems with tariff incentives. *Appl. Energy* **2017**, *203*, 422–441. [CrossRef]
24. Samuel, O.; Almogren, A.; Javaid, A.; Zuair, M.; Ullah, I.; Javaid, N. Leveraging blockchain technology for secure energy trading and least-cost evaluation of decentralized contributions to electrification in Sub-Saharan Africa. *Entropy* **2020**, *22*, 226. [CrossRef]
25. Samuels, J.A.; Ahile, T.; Booysen, M. Energy Usage Measurements for Public Schools in Western Cape, South Africa. 2024. Available online: https://data.mendeley.com/datasets/nm2vc4v2br/1 (accessed on 23 August 2025).
26. Eskom; Stellenbosch University; University of Cape Town. Domestic Electrical Load Metering 1994–2014. 2014. Available online: https://www.datafirst.uct.ac.za/dataportal/index.php/catalog/760 (accessed on 23 August 2025).
27. Stratford, H.; Booysen, M.J. Electrifying Last-Mile Delivery Motorcycles in Cape Town: Challenges and Opportunities. *Preprint* **2025**. Available online: https://www.preprints.org/manuscript/202510.0719 (accessed on 14 January 2026).
28. National Renewable Energy Laboratory. System Advisor Model™ (SAM™) Version 16 April 2025. Available online: https://sam.nrel.gov (accessed on 23 August 2025).
29. Soto, A.; Berrueta, A.; Mateos, M.; Sanchis, P.; Ursúa, A. Impact of micro-cycles on the lifetime of lithium-ion batteries: An experimental study. *J. Energy Storage* **2022**, *55*, 105343. [CrossRef]
30. Pereira, J.L.J.; Oliver, G.A.; Francisco, M.B.; Cunha, S.S., Jr.; Gomes, G.F. A review of multi-objective optimization: Methods and algorithms in mechanical engineering problems. *Arch. Comput. Methods Eng.* **2022**, *29*, 2285–2308. [CrossRef]
31. Sharma, S.; Kumar, V. A comprehensive review on multi-objective optimization techniques: Past, present and future. *Arch. Comput. Methods Eng.* **2022**, *29*, 5605–5633. [CrossRef]
32. Madanchian, M.; Taherdoost, H. A comprehensive guide to the TOPSIS method for multi-criteria decision making. *Madanchian Taherdoost Compr. Guide Topsis Method Multi-Criteria Decis. Making. Sustain. Soc. Dev.* **2023**, *1*, 2220. [CrossRef]
33. Nguyen, H.Q.; Nguyen, V.T.; Phan, D.P.; Tran, Q.H.; Vu, N.P. Multi-Criteria Decision Making in the PMEDM Process by Using MARCOS, TOPSIS, and MAIRCA Methods. *Appl. Sci.* **2022**, *12*, 3720. [CrossRef]

Disclaimer/Publisher's Note: The statements, opinions and data contained in all publications are solely those of the individual author(s) and contributor(s) and not of MDPI and/or the editor(s). MDPI and/or the editor(s) disclaim responsibility for any injury to people or property resulting from any ideas, methods, instructions or products referred to in the content.